Desalination and Water Treatment
www.deswater.com

doi: 10.5004/dwt.2017.21352

89 (2017) 47–52
September

Performance of combined anoxic–aerobic fluidized bed bioreactors for the domestic wastewater treatment

Yangyang Feng*, Lei Zhang, Xiaoming Hu

School of Pharmaceutical Sciences, Nanjing Tech University, Nanjing 211800, China, Tel. +86 25 83313960; emails: yangyangfeng@njtech.edu.cn (Y. Feng), leizhang@njtech.edu.cn (L. Zhang), xmhu83@126.com (X. Hu)

Received 23 February 2017; Accepted 20 August 2017

ABSTRACT

Fluidized-bed bioreactors (FBBRs) have attracted considerable interest as an alternative to the conventional suspended growth and fixed-film wastewater treatment processes because of the high performance efficiency. In this study, a laboratory-scale combined anoxic–aerobic FBBR with porous magnetic ceramics as carrier was developed to treat domestic wastewater. During the 120-d steady period, the hydraulic retention time decreased from 2.8 to 1.6 h; the effluent chemical oxygen demand (COD_{cr}), ammonia nitrogen (NH_4–N) and total nitrogen (TN) were below 25, 3.2 and 11.4 mg/L, respectively. The results demonstrated that the COD_{cr}, NH_4–N and TN removal efficiencies were 15%–20% higher than other biologic processes. Furthermore, near-complete removal of excess sludge was obtained, the system sludge yield coefficient of the system was 0.233 g VSS/g COD_{cr}, far less than the case with other biologic processes.

Keywords: Anoxic–aerobic; Domestic wastewater; Fluidized-bed bioreactor; Porous magnetic ceramics

1. Introduction

With the development of urbanization, the quantity of domestic wastewater is increased greatly and wastewater pollution is an important issue to be resolved. However, there are some problems in existing wastewater treatment processes, such as space limitations, more strict effluent standard, and higher processing costs. It is imperative to develop efficient wastewater treatment technologies with lower energy exhaustion, higher efficiency, and less covering area.

The fluidized-bed bioreactor (FBBR) combines the fluidization technology, activated sludge process, and biofilm process has been applied extensively to chemical and biochemical processes [1–3]. Compared with traditional biologic treatments, the FBBR presents several advantages, such as high biomass retention, small footprint, and low hydraulic residence time (HRT) [4–7]. This technology also combines the more compact and efficient fixed-film process with the wastewater treatment process.

To date, the FBBR has been reported in various studies to be suitable for different wastewater treatments. In previous studies, various organic and inorganic materials were also successfully applied as carriers in FBBR, such as lava rock, activated carbon, natural zeolite, polyurethane and polystyrene [8–12]. These results demonstrated that the fluidization increases the mass-transfer efficiency and overcomes operating problems such as bed clogging and short-circuiting. Meanwhile, the large surface area of carriers can ensure a high biomass concentration and efficient immobilization of slow-growing microorganism. These factors can facilitate the microbial biomass colonization and increase efficiency of treatment.

However, some crucial parameters restrict the widespread application of this technology, such as carrier material selection, establishment of bioreactor operating conditions, and irreversible biofilm formation in a short time period. Therefore, novel magnetic porous ceramics were prepared and employed in the rapid mass-transfer anoxic–aerobic FBBR as carriers. The present study aims to investigate the properties of the porous carrier, the quick start-up of the

* Corresponding author.

bioreactor, and the performance of the FBBR for domestic wastewater treatment.

2. Materials and methods

2.1. Domestic wastewater

Domestic wastewater was collected from Suojin wastewater plant (Nanjing, China). The main characteristics of domestic wastewater were chemical oxygen demand (COD; 300 ± 50 mg/L), NH_4–N (45 ± 10 mg/L), total nitrogen (TN; 60 ± 10 mg/L), suspend solid (310 ± 60 mg/L), pH 7.0.

2.2. Magnetic porous carrier

The magnetic porous ceramics were processed as follows. The raw materials used were Ca-bentonite, coal ash, activated carbon (as a pore-forming agent) and magnetite Fe_3O_4 (as the magnetic seed) at a 12:6:1:1 ratio (w/w). A quantity of 200 mL water and 5 mL polyethylene glycol per 1,000 g raw materials were added. Then, the samples were dried at 105°C until the weight invariant, subsequently, sintered at 1,100°C for 1 h in an electric furnace (Model ZGRS-160/2.55, China).

2.3. Reactor configuration and operation

Fig. 1 shows a schematic diagram of the lab-scale combined anoxic–aerobic FBBRs. The working volume of the anoxic zone was 2.8 L, consisted of a 77.0 cm length by 7.0 cm diameter acrylic outer column and a 71.0 cm length by 3.4 cm diameter acrylic inner column. While the working volume of the aerobic zone was 7.2 L, with the sizes of the outer and inner column were 75.0 cm length by 11.0 cm diameter and 71.0 cm length by 5.9 cm diameter, respectively. The upper end of the bioreactor was equipped with a gas–liquid–solid separator and an inclined plate separator to reduce the liquid velocity and prevent particle loss. A cone was installed at the lower part of the outer cylinder at a 55° inclined angle to attain smooth particle circulation.

The FBBRs were carried out at room temperature (about 25°C). The anoxic and aerobic bioreactors were inoculated with 1.6 and 3.2 L activated sludge obtained from Jinzhou wastewater treatment plant (Nanjing, China). The mixed liquid suspended solids of anoxic and aerobic bioreactors were 6.7 and 5.8 g/L, respectively. The effluent was recycled through a recycling pump connecting the effluent outlet and the feed inlet during operation. In the upflow area, high fluidization increased liquid–solid interface turbulence intensity. Meanwhile, the carriers rapidly fall under gravity due to the high density in the downflow area, thereby increasing the solid–liquid phases mass transfer rate. Consequently, the mass-transfer rate and removal efficiency of the whole system was increased.

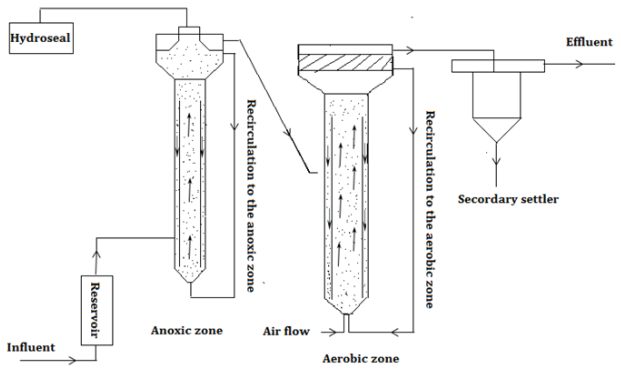

Fig. 1. Schematic diagram of the lab-scale combined anoxic–aerobic FBBRs.

The FBBRs operation stage was initiated with a 1.9 kg COD/m^3 d and a HRT value of 3.2 h. The COD_{cr}, NH_4–N and TN concentrations of influent were 300, 50 and 50 mg/L, respectively. After 10 d operation, the COD_{cr}, NH_4–N and TN concentrations of effluent were 36, 0.28 and 9 mg/L, respectively. Then, progressive increase of the organic loading was applied. During the entire 120-d operation period, the system was operated under four different operational conditions with varying organic load rate (OLR) values from 2.6 kg COD_{cr}/(m^3·d) to 4.2 kg COD_{cr}/(m^3·d) (2.6, 3.1, 3.6 and 4.2 kg COD/(m^3·d)) and varying HRTs from 2.8 to 1.6 h (2.8, 2.4, 2 and 1.6 h) accordingly.

2.4. Biomass growth kinetics study

The study of biomass growth kinetics was calculated using the data obtained from the domestic wastewater treatment research. The kinetic form of the Prit's maintenance energy model [13,14] was employed for the determination of the growth kinetics coefficients by Eqs. (1)–(3), such as sludge yield (y), maintenance energy coefficient (E), and substrate (COD_{cr}) utilization rate (r_s):

$$r_s = \frac{S_0 - S}{\tau} \tag{1}$$

$$E = \frac{S_0 - S}{\tau X} - \frac{1}{\tau_P y} = \frac{r_s}{X} - \frac{1}{\tau_P y} \tag{2}$$

$$\frac{r_s}{X} = \frac{1}{y}\frac{1}{\tau_p} + E \tag{3}$$

where τ_p = sludge retention time, h; SRT = (volume of aerobic FBBR)/(discharged sludge); τ = HRT, h; r_s = substrate (COD_{cr}) utilization rate, g COD_{cr}/L h; S_0 = Initial COD_{cr} concentration, g/L; S = COD_{cr} concentration after time τ, g/L; X = biomass concentration, g VSS/L; E = maintenance energy coefficient, g COD_{cr}/g VSS h; y = sludge yield, g VSS/g COD_{cr}.

2.5. Analytical methods

Samples were collected from influent, anoxic effluent and final effluent in airtight sample bottles and refrigerated at 4°C prior to analysis. NH_4–N was measured using an ion chromatography (DIONEX120, USA). The COD_{cr}, volatile suspended solids (VSS) and pH were measured according to standard methods [15]. The TN test was according to alkaline potassium persulfate method using ultraviolet spectrophotometry [16]. The structural analyses of porous carrier and the biofilm were conducted by a scanning electron microscope (SEM; JSM-5900, Japan) [17]. Magnetic field strength was measured by a gauss meter (Lake Shore-475, USA). The compressive strength was tested by a flexural strength tester

(HK-403, China). The porosity of the carrier was measured by the Archimedes method [18]. Biomass adhesion to the carrier particles was determined according to the method of Chen and Chen [19]. The specific surface area of the carrier was tested with Monosorb-type apparatus (Quantachrome, USA) using single point BET method.

3. Results and discussion

3.1. Porous ceramics characterization

The physical and chemical characterizations of porous magnetic carrier were exhibited as in Table 1. The SEM image (Fig. 2) shows that the magnetic carrier surface was rough, porous and with large surface area. There were a lot of uneven crevices and pores on the carriers, with the pore diameter between 50 and 200 μm.

3.2. SEM analyses

The colonization and growth of the biomass on the porous magnetic ceramics was observed via SEM. It can be seen from Fig. 3 that both anoxic and aerobic bacteria showed high affinity to adsorb and form colonies on the porous ceramics. The biofilm is well attached and apparently spread on the pores by the extracellular polymeric substances. These were attributed to the rough surface, porous structure and large specific area of the carrier beads available for biomass retention, thereby increasing the available area for biofilm development. The amount of biomass adhering to the porous ceramics reached 27.8 mg VSS/g in the anoxic zone, while 36.5 mg VSS/g in the aerobic zone.

The SEM image also showed that well biofilm structure was maintained on the interior of carriers. The difference of biofilm morphology in anoxic and aerobic zones was obvious. In the anoxic zone, the biofilm was mainly composed of sphere bacteria, bacillus and slice bacteria. While in the aerobic zone, the bacillus and filamentous bacteria were the observed dominant microbes.

3.3. Performance of anoxic–aerobic FBBRs

The FBBRs were operated with a low OLR value of 1.9 kg COD_{cr}/m^3 d and an HRT value of 3.2 h, which was much more suitable for biomass colonization and growth. The system could work effectively only after 10 d from the start-up. The COD_{cr} and NH_4–N concentrations of effluent were 36 and 0.28 mg/L, respectively.

Table 1
Physical and chemical characterizations of porous magnetic carrier

Particle size (mm)	0.4–0.8
Bulk density (g/cm^3)	1.72
Porosity (%)	51.24
Compressive strength (MPa)	6.0–6.5
Magnetic field intensity (mG)	80–90
Specific surface area (m^2/g)	43.52

After 10 d start-up, the FBBRs were steady operated under four different operational conditions with the OLR value increased from 2.6 kg $COD_{cr}/(m^3 \cdot d)$ to 4.2 kg $COD_{cr}/(m^3 \cdot d)$ (2.6, 3.2, 3.6 and 4.2 kg $COD_{cr}/(m^3 \cdot d)$) and HRT varying from 2.8 to1.6 h (2.8, 2.4, 2.0 and 1.6 h) accordingly. Fig. 4 shows the COD_{cr} removal efficiency of FBBRs during the 120 d steady operation. The FBBRs showed a strong resistance to the shocked OLR, with the system OLR value varied from 2.6 kg $COD_{cr}/(m^3 \cdot d)$ to 4.2 kg $COD_{cr}/(m^3 \cdot d)$, the COD removal efficiency was stably above 91%, and the effluent COD_{cr} was below 25 mg/L.

The NH_4–N concentration of influent was between 33 and 48 mg/L. The FBBRs show a good NH_4–N removal efficiency during the whole steady period. The first two phases with the HRT values of 2.8 and 2.4 h, the NH_4–N removal efficiency reached up to 99%, and the effluent NH_4–N was below 0.3 mg/L. In phases 3 and 4, the NH_4–N removal efficiency decreased to 93%–96%, the NH_4–N concentration of effluent raised to 3.2 mg/L (illustrated as Fig. 5). These were attributed to the reduction of the HRT.

The TN concentration of effluent ranged from 39 to 51 mg/L during the steady period. The TN removal efficiency was between 83% and 86% in stage 1 and phase 2. However, with the HRT reduction, the TN removal efficiency was

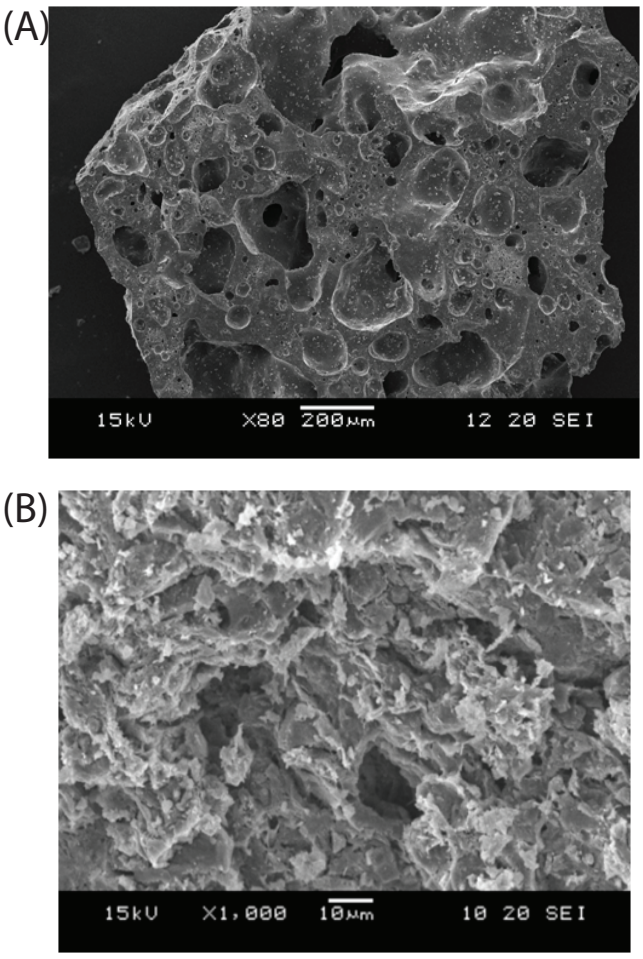

Fig. 2. SEM image of the porous magnetic carrier; (A) the surface; (B) the interior.

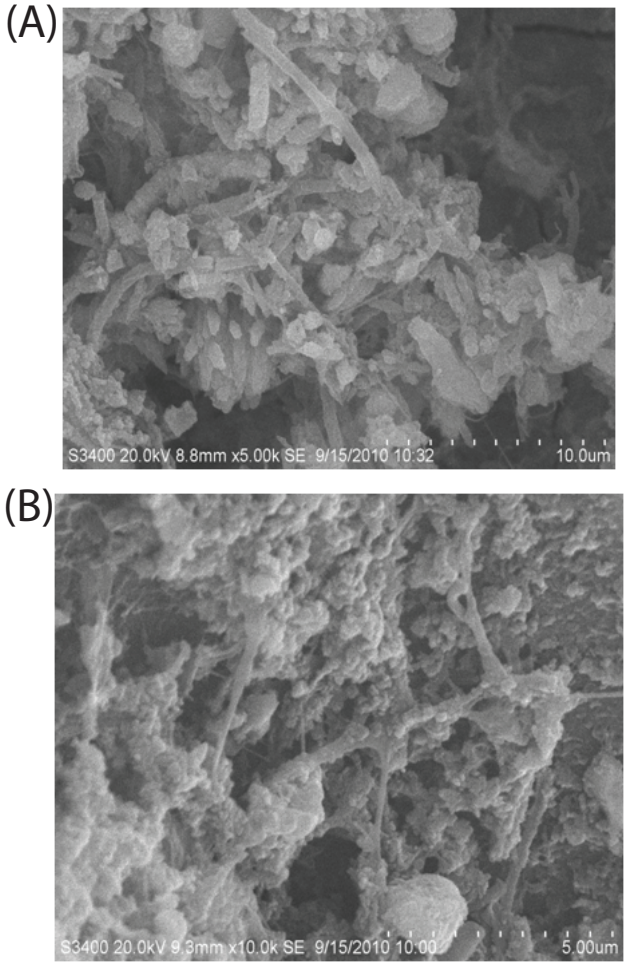

Fig. 3. SEM images of biofilms adsorbed on the inner of porous carrier; (A) aerobic zone, (B) anoxic zone.

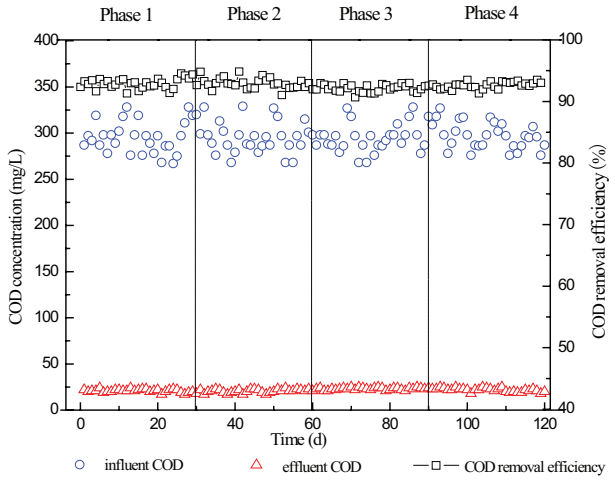

Fig. 4. COD removal efficiency of FBBRs during the steady operation period.

decreased to 78% and 73% in the last two phases (Fig. 6). The results illustrated that the varying OLR had a negative effect on the TN removal efficiency.

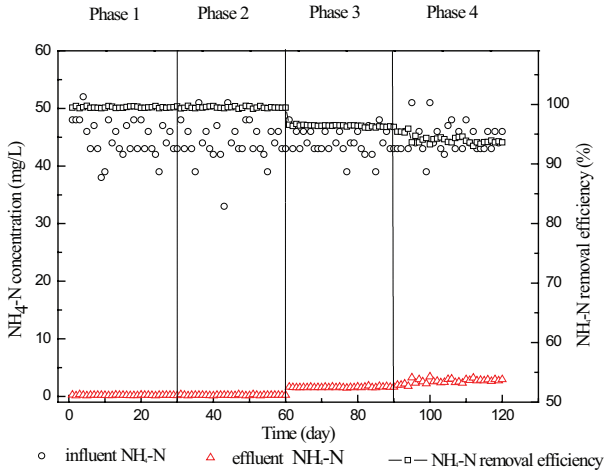

Fig. 5. NH_4–N removal efficiency of the FBBRs during the steady period.

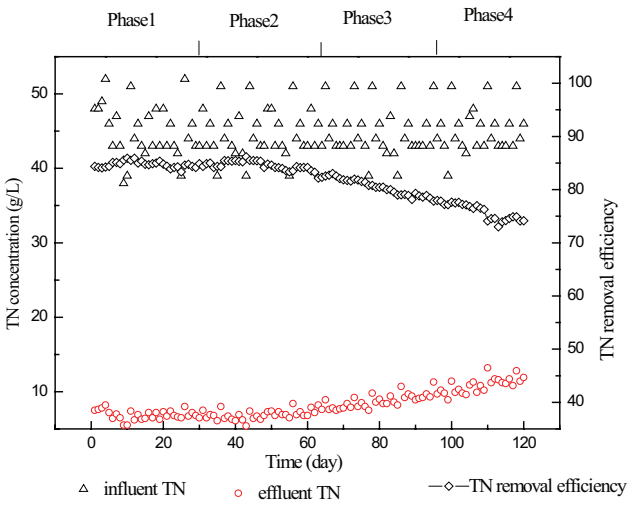

Fig. 6. TN removal efficiency of steady period.

3.4. Biomass growth kinetics study

The plot of r_s/X vs. $1/\tau_p$ (from Eq. (3)) yielded a straight line whose slope gave the reciprocal of sludge yield coefficient (y) and intercept gave the maintenance energy coefficient (E; Fig. 7).

The plot revealed the sludge yield coefficient (y) and maintenance energy coefficient (E) to be 0.23 g VSS/g COD_{cr} and 0.015 g COD_{cr}/g VSS h, which suggested a healthy growth pattern of the microorganisms attached to the interior pores of the carriers with a low excess sludge rate.

Compared with other domestic wastewater biological treatment processes (Table 2) [20–24], the FBBR demonstrated several advantages, including COD_{cr}, NH_4–N and TN removal efficiencies were 20% higher than other biologic processes; the HRT was 60% shorter than other processes; and the excess sludge yield was 50% less than other processes.

The good treatment efficiency of FBBRs was attributed to the inherent advantages of FBBR and carrier. The fast

Table 2
Comparison of different domestic wastewater biotreatment efficiency

Biotreatment processes	HRT (h)	COD removal efficiency (%)	NH_3–N removal efficiency (%)	TN removal efficiency (%)	y (g VSS/g COD)
Active sludge	6–8	80–85	50–60	25–35	0.6
Sequencing batch reactor	6–8	85–90	80–90	55–65	0.45
Cyclic activated sludge system	4–6	80–85	80–85	60–65	0.45
A^2/O	10–14	85–90	65–80	60–65	0.40
A/O	3–6	85–90	50–60	50–60	–
This study	1.6–2.8	91–95	93–99	73–86	0.23

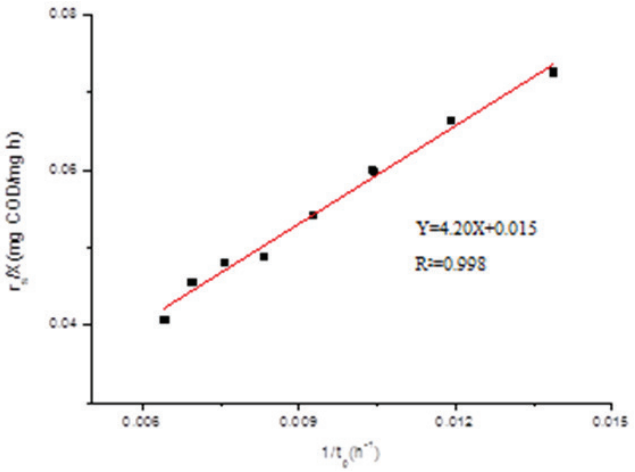

Fig. 7. Kinetics of biomass growth.

fluidization provided high mass transfer, uniform mixing; and maximized interphase contact efficiency between biofilm and organic substrate. The porous structure and large surface area of ceramics carrier were propitious to biomass attached proliferation and also achieved high biomass concentrations through porous canals. Furthermore, the immobilized biofilm exhibited high biodegradation activity, it also might be attributed to the influence of micro-magnetic fields on biological functions of the biofilm by changes in hormones, activity of some enzymes, and membrane ion transport, and these could reduce or eliminate mass transfer problems to improve the biodegradation activities [25,26]. The physical and chemical properties of wastewater were beneficial for degradation of organic compounds after magnetization.

4. Conclusion

The combined anoxic–aerobic FBBRs were successfully employed to the domestic wastewater treatment in this study. Good treatment efficiencies were obtained. During the 120-d steady period, with varying HRT values from 2.8 to1.6 h, high removal efficiencies were in terms of COD_{cr} (91%–95%), NH_4–N (93%–99%) and TN (73%–86%).

In the combined anoxic–aerobic FBBRs, the carriers were distributed equally in the entire bioreactor under fast fluidization condition, and the working volume, mass transfer rate and treatment efficiencies of the bioreactor were significantly enhanced. Compared with other biological treatment processes, the FBBRs present a number of advantages, such as 20% higher removal efficiencies, 60% shorter HRT, and 50% lower excess sludge yield. These results demonstrated that FBBR is a potential process for domestic wastewater treatment.

Acknowledgments

The present work was partly carried by the National Natural Science Foundation of China (No. 51608261).

References

[1] M.M. Bello, A.A.A. Raman, M. Purushothaman, Applications of fluidized bed reactor in wastewater treatment – a review of the major design and operational parameters, J. Cleaner Prod., 141 (2016) 1492–1514.
[2] Y. Feng, B. Lu, Y. Jiang, Y. Chen, S. Shen, Performance evaluation of anaerobic fluidized bed reactors using brick beads and porous ceramics as support materials for treating terephthalic acid wastewater, Desal. Wat. Treat., 53 (2015) 1814–1821.
[3] J.K. Braga, F. Motteran, E.L. Silva, M.B.A. Varesche, Evaluation of bacterial community from anaerobic fluidized bed reactor for the removal of linear alkylbenzene sulfonate from laundry wastewater by 454-pyrosequence, Ecol. Eng., 82 (2015) 231–240.
[4] S. Gabardo, R. Rech, M.A.Z. Ayub, Performance of different immobilized-cell systems to efficiently produce ethanol from whey: fluidized batch, packed-bed and fluidized continuous bioreactors, J. Chem. Technol. Biotechnol., 87 (2012) 1194–1201.
[5] F.D. Capua, A.M. Lakaniemi, J.A. Puhakka, P.N.L. Lens, G. Esposito, High-rate thiosulfate-driven denitrification at pH lower than 5 in fluidized-bed reactor, Chem. Eng. J., 310 (2016) 282–291.
[6] M. Andalib, G. Nakhla, J. Zhu, High rate biological nutrient removal from high strength wastewater using anaerobic-circulating fluidized bed bioreactor (A-CFBBR), Bioresour. Technol., 118 (2012) 526–535.
[7] P. Rungkitwatananukul, S. Nomai, Y. Hirakata, W. Pungrasmi, C. Puprasert, Microbial community analysis using MiSeq sequencing in a novel configuration fluidized bed reactor for effective denitrification, Bioresour. Technol., 221 (2016) 677–681.
[8] N. Fernandez, S. Montalvo, R. Borja, L. Guerrero, E. Sanchez, I. Cortes, M.F. Colmenarejo, Performance evaluation of an anaerobic fluidized bed reactor with natural zeolite as carrier material when treating high-strength distillery wastewater, Renew. Energy, 33 (2008) 2458–2466.
[9] A.R. Barros, M.A.T. Adorno, I.K. Sakamoto, S.I. Maintinguer, M.B.A. Varesche, E.L. Silva, Performance evaluation and phylogenetic characterization of anaerobic fluidized bed reactors using ground tire and pet as carrier materials for biohydrogen production, Bioresour. Technol., 102 (2011) 3840–3847.
[10] D.W. Gao, Q. Hua, C. Yao, N.Q. Ren, W.M. Wu, Integrated anaerobic fluidized-bed membrane bioreactor for domestic wastewater treatment, Chem. Eng. J., 240 (2014) 362–368.

[11] X. Chen, L. Kong, X. Wang, S. Tian, Y. Xiong. Accelerated start-up of moving bed biofilm reactor by using a novel suspended carrier with porous surface, Bioproc. Biosyst. Eng., 38 (2015) 273–285.
[12] G. Zou, S. Papirio, A.M. Lakaniemi, S.H. Ahoranta, J.A. Puhakka, High rate autotrophic denitrification in fluidized-bed biofilm reactors, Chem. Eng. J., 284 (2016) 1287–1294.
[13] S.J. Prit, The maintenance energy of bacteria in growing cultures, Proc. R. Soc. Lond. Ser., 163 (1965) 224–231.
[14] S.J. Prit, Maintenance energy: a general model for energy-limited and energy sufficient growth, Arch. Microbiol., 133 (1982) 300–302.
[15] APHA, Standards Methods for the Examination of Water and Wastewater, American Public Health Association, American Water Works Association, Water Pollution Control Federation, Washington, D.C., USA, 2002.
[16] L. Zhang, S. Zhang, Y. Peng, X. Han, Y. Gan, Nitrogen removal performance and microbial distribution in pilot- and full-scale integrated fixed-biofilm activated sludge reactors based on nitritation-anammox process, Bioresour. Technol., 196 (2015) 448–453.
[17] M.B. Varesche, M. Zaiat, L.G.T. Vieira, R.F. Vazoller, E. Foresti, Microbial colonization of polyurethane foam matrices in horizontal-flow anaerobic immobilized-sludge reactor, Appl. Microbiol. Biotechnol., 48 (1997) 534–538.
[18] E.J. Lee, Y.H. Koh, B.H. Yoon, H.E. Kim, H.W. Kim, Highly porous hydroxyapatite bioceramics with interconnected pore channels using camphene-based freeze casting, Mater. Lett., 60 (2007) 2270–2273.
[19] C.Y. Chen, S.D. Chen, Biofilm characteristics in biological denitrification biofilm reactors, Water Sci. Technol., 41 (2000) 147–154.
[20] Y.J. Chan, M.F. Chong, C.L. Law, D.G. Hassell, A review on anaerobic–aerobic treatment of industrial and municipal wastewater, Chem. Eng. J., 155 (2009) 1–18.
[21] W. Zeng, L. Li, Y.Y. Yang, S.Y. Wang, Y.Z. Peng, Nitritation and denitritation of domestic wastewater using a continuous anaerobic–anoxic–aerobic (A2O) process at ambient temperatures, Bioresour. Technol., 101 (2010) 8074–8082.
[22] Y.Q. Liu, B.Y.P. Moy, J.H. Tay, COD removal and nitrification of low-strength domestic wastewater in aerobic granular sludge sequencing batch reactors, Enzyme Microb. Technol., 42 (2007) 23–28.
[23] A. Tawfik, M. Sobhey, M. Badawy, Treatment of a combined dairy and domestic wastewater in an up-flow anaerobic sludge blanket (UASB) reactor followed by activated sludge (AS system), Desalination, 227 (2008) 167–177.
[24] M.A. Fulazzaky, N.H. Abdullah, A.R.M. Yusoff, E. Paul, Conditioning the alternating aerobic-anoxic process to enhance the removal of inorganic nitrogen pollution from a municipal wastewater in France, J. Cleaner Prod., 100 (2015) 195–201.
[25] B. Jiang, Z.C. Zhou, Y. Dong, B. Wang, J. Jiang, X. Guan, S. Gao, A. Yang, Z. Chen, H. Sun, Bioremediation of petrochemical wastewater containing BTEX compounds by a new immobilized bacterium *Comamonas* sp. JB in magnetic gellan gum, Appl. Biochem. Biotechnol., 176 (2015) 572–581.
[26] T.T. Le, K. Murugensan, C.S. Lee, C.H. Vu, Y.S. Chang, J.R. Jeon, Degradation of synthetic pollutants in real wastewater using laccase encapsulated in core-shell magnetic copper alginate beads, Bioresour. Technol., 216 (2016) 203–210.